

Modelling the Fringing of the ACS CCD Detectors

J. R. Walsh, N. Pirzkal & A. Pasquali

*Space Telescope European Co-ordinating Facility, European Southern Observatory,
Karl-Schwarzschild Strasse 2, D-85748 Garching, Germany*

Abstract. The fringing of CCD detectors occurs because of interference between the incident light and the light internally reflected at the interfaces between the thin layers of the CCD chip. Knowing the construction of the CCD, namely the materials composing the layers, their refractive index variation with wavelength and their thicknesses, the resulting fringe amplitude can be calculated from geometrical optics. Malamuth et al. have applied this technique to the STIS CCD. The topmost layer controls the high frequency fringes and the lower layers the envelope of the fringing amplitude with wavelength. Modelling of the four-layer structure of the ACS CCDs is described. The High Resolution Channel (SiTe) CCD is a copy of the STIS one and so has a similar structure, but the Wide Field Channel (also SiTe) chip has proprietary construction. The observed fringe amplitude across the CCD is used to predict the spatial variation of the thickness of the top layer, whilst the thicknesses of the lower layers are kept fixed. By applying the model maps of the layer thicknesses, the observed fringing in ACS can be strongly reduced from peak-to-peak of >20% to a few percent.

1. Fringing in CCDs

Interference in the CCD detection layer between incident light and that reflected from interfaces of the thin layers leads to fringing. As the silicon layer becomes more transmissive in the red, so more signal is contributed by internally reflected light. The fraction of light internally reflected depends on the number of layers of the CCD, their thickness and material, which enters through the complex refractive index, and the wavelength of the incident light. Knowing in detail the bulk construction of the CCD, the resulting fringe amplitude can be calculated from geometrical optics. The refractive index generally varies as a function of wavelength for most materials (Palik 1985), and is a key ingredient for the optical modelling. Malamuth et al. (2000; 2002) successfully applied this technique to the STIS CCD. By matching the observed fringe amplitudes across the CCD, the thicknesses of the layers can be modelled using tabulated refractive indices, although Malamuth et al. found that the bulk Si refractive index had to be adjusted over some wavelength range to obtain a satisfactory fit. Here we apply the fringe modelling technique to the ACS thinned, backside-illuminated CCDs.

2. ACS High Resolution Channel

The ACS High Resolution Channel (HRC) CCD is a SiTe STIS spare, so was modelled closely following the Malamuth et al. parameters for STIS. It is composed of 4 layers as shown in Figure 1 (left). The lower 3 layers combine to modulate the envelope of the fringe amplitude, whilst the top Si (detection) layer produces the high frequency fringing. The optical modelling is performed by summation of the amplitudes of the E-vectors for the incident and 4 returned rays at a grid of wavelengths, as for multi-layer coatings (cf. Born

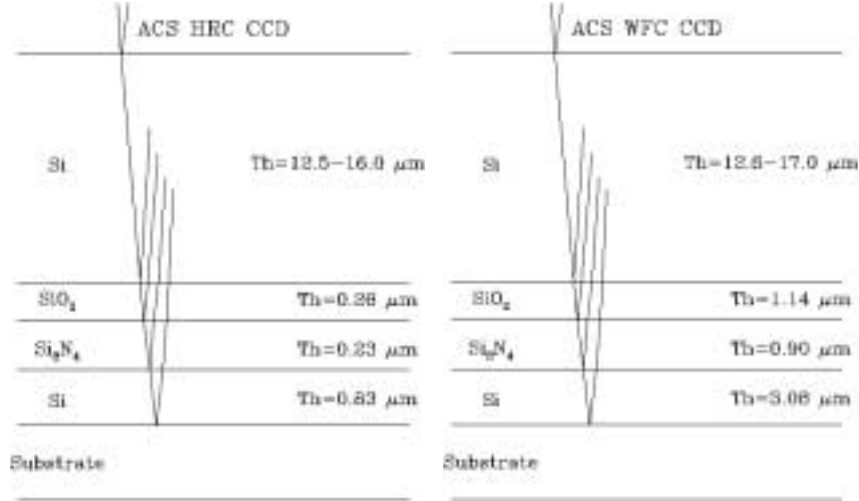


Figure 1. The layer structure of the ACS High Resolution Channel SITE CCD is shown in the left panel and the assumed layer structure of the ACS Wide Field Channel SITE CCD in the right panel.

& Wolf, p. 627). The data with which to compare the model consisted of 37 continuum lamp images taken with the RASCAL simulator, illuminated by a monochromator (20 Å bandpass), whilst the ACS was under ground testing at Goddard. ACS has no on-board facility for narrow band illumination, so ground calibration was critical. The function to be minimized (rms of observed-predicted fringe amplitude as a function of layer thickness) is highly periodic and several passes were required to locate the minimum. An amplitude factor, to allow for the fact that the geometrical optics model is not exact in terms of transmissions and reflectivities of the layer interfaces, was also applied, but was taken as a constant. Figure 2 shows the model compared with the observed monochromatic fringe amplitudes at the chip center. The 1024^2 image of the layer thickness of the HRC Si layer was used to compute a model fringe map for direct comparison with the observed data.

Figure 3 (left) shows the observed fringing map at 9200 Å. In the fitting procedure, the influence of the 2nd layer (SiO_2) was investigated by varying its thickness using the initial map of the 1st (Si) layer (Figure 1). It was found that there is little to be gained by using a pixel-by-pixel fit to the thickness of the 2nd layer. This is clear from the Figure 3 (right), which shows the observed fringing and the residuals after correcting by the model, where the traces across the CCD were formed by averaging two rows (511–512). The strong reduction in the observed fringing demonstrates the effectiveness of the fringe modelling as applied to the HRC chip.

3. Wide Field Channel

The Wide Field Channel (WFC) has two 4096×2048 SITE back-illuminated chips using MPP technology, but of proprietary construction. No layer thickness or materials data were available. The same 4 layer model as for the HRC chip was however assumed and the thicknesses of the layers to match the observed fringing were similarly modelled (see Figure 1, right).

46 monochromatic flats were taken during ground testing at Goddard, of width 20 and 10 Å, and the minimum rms of the observed-model fringe amplitude was better defined than for the HRC. By minimizing the rms for each layer separately, a satisfactory fit for the chip structure could be found (see Figure 1). Keeping the thickness of the layers 2–4

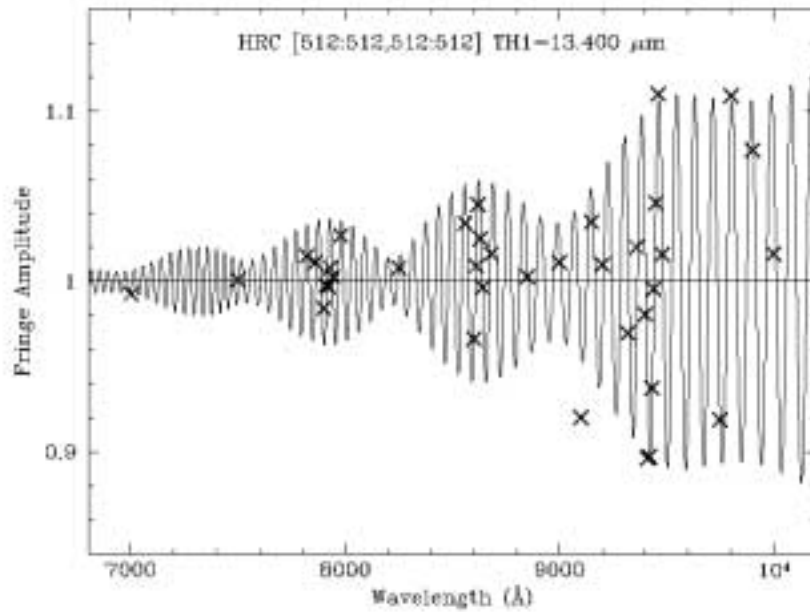


Figure 2. The model fringing (continuous line) is shown for a 2×2 pixel area at the center of the HRC chip with the observed fringe amplitude, displayed by crosses, as a function of wavelength.

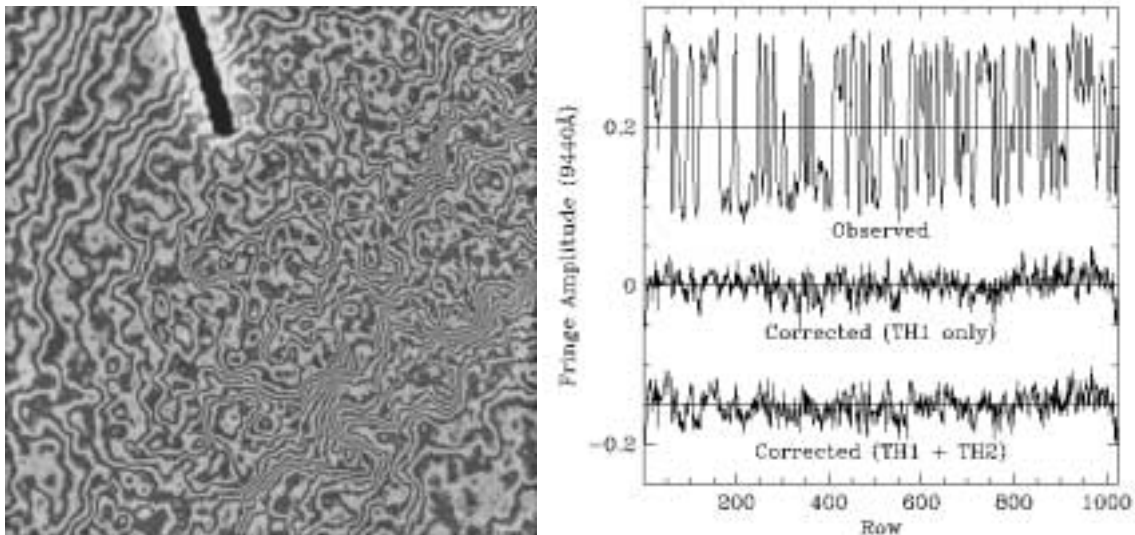


Figure 3. In the left panel is shown the observed fringing map at 9200 \AA ; the peak amplitude is 0.15. In the right panel, the observed fringing at 9440 \AA (upper trace) is compared with the result of correcting the observed fringing by the model using the pixel-to-pixel fit to the top CCD layer only (middle) and for the fit with a pixel-by-pixel fit of the top two layers (bottom).

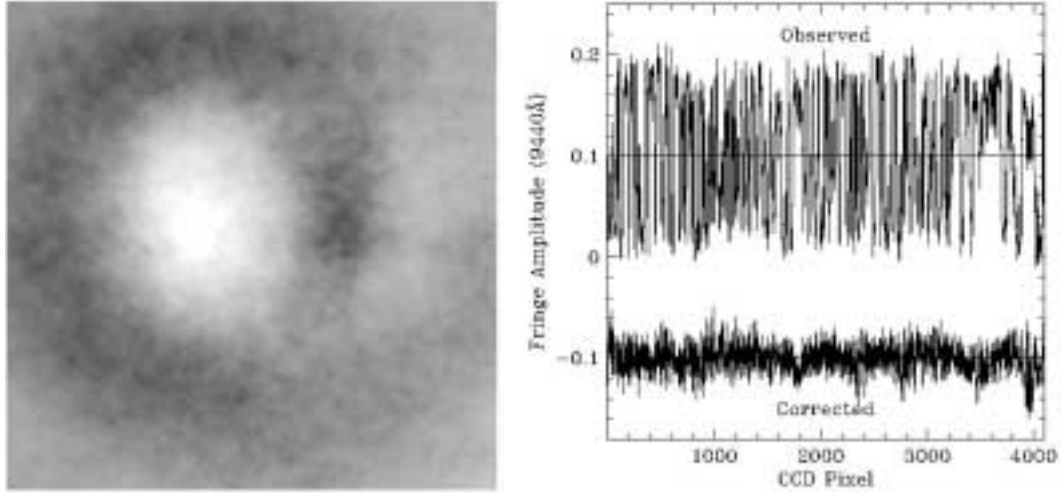


Figure 4. In the left panel, the modelled layer thickness of the top layer of the WFC CCD (limits 12.61 to 17.13 μm) is shown with the two chips butted together. The right panel shows the observed fringing at 9440 \AA (upper trace) compared with the result of correcting the observed fringing by the model (lower trace).

fixed, the observed fringing of the 46 flats was modelled as a function of Layer 1 (assumed to be Si) thickness. The result is shown in Figure 4 (left); the sampling is 1×1 pixels and the ‘cosmic doughnut’ familiar from flat field images is apparent. Comparing model fringe maps with observed shows good agreement; correcting the observed fringing by the model can reduce the amplitude of fringing from 0.12 to ~ 0.03 (see Figure 4 right for row 1021 of CHIP2).

So far no detectable fringing has been found in WFC 1st order spectra. This is because the PSF modulates the fringing of the slitless spectra over the range of ~ 2 pixels (80 \AA) reducing it to \sim few %. For the HRC the detectable fringing for point sources is larger since the pixels are narrower in wavelength (27 \AA in 1st order).

4. Correction for Fringing

The fits to the CCD layer thickness will be incorporated in the ACS slitless spectra reduction package, aXe (Pirzkal et al. 2001), to effectively reduce observed fringing in extracted spectra. When wavelength is assigned to a pixel in an extracted slitless spectrum, the fringe amplitude is computed from the model and the observed signal corrected.

This fringe modelling method is quite general and can be applied to any CCD, given specification of its layer structure and a set of monochromatic flat fields over the wavelength range of significant fringing. Malumuth (this volume, p. 197) has applied the method to the WFC3 CCDs.

References

- Born, M. & Wolf, E. 1975, *Principles of Optics*, 5th ed.
 Malumuth, E. M., Hill, R. S., Gull, T. R., et al. 2000, AAS, 197, 1204
 Malumuth, E. M., Hill, R. S., Gull, T. R., et al. 2002, AJ, in press
 Palik, E. D. 1985, *Handbook of Optical Constants of Solids*
 Pirzkal, N., Pasquali, A., & Demleitner, M., 2001, ST-ECF Newsletter, No. 29, p. 5.